*Article*

# Effects of NaHSO₃ on Cellular Metabolic Energy, Photosynthesis and Growth of *Iris pseudacorus* L.

**Tian Chen [1], Yanyou Wu [2],\*, Deke Xing [1],\* and Rongrong Duan [1]**

[1] Key Laboratory of Modern Agricultural Equipment and Technology, Ministry of Education, Institute of Agricultural Engineering, Jiangsu University, Zhenjiang 212013, China; 2211916001@stmail.ujs.edu.cn (T.C.); 2211916002@stmail.ujs.edu.cn (R.D.)

[2] Research Center for Environmental Bio-Science and Technology, State Key Laboratory of Environmental Geochemistry, Institute of Geochemistry, Chinese Academy of Sciences, Guiyang 550081, China

\* Correspondence: wuyanyou@mail.gyig.ac.cn (Y.W.); xingdeke@ujs.edu.cn (D.X.)

**Abstract:** According to the law of energy conservation, the energy consumed by plants to resist adversity is equal to the difference between photosynthetic energy and growth energy consumption and cellular metabolic energy in plants. The cellular metabolic energy is calculated based on the electrical signals in plants. This study mainly investigated the effect of NaHSO₃ on the growth and energy traits of the aquatic plant *Iris pseudacorus* L. and explored the effect of NaHSO₃ on energy consumption in the process of plant development. In this study, NaHSO₃ was used for simulating sulfur pollution in water medium. During the 20-day experiment period, the response of *I. pseudocorus* to the polluted water sources simulated by adding different concentrations of NaHSO₃ (0, 0.5, 2, 4, 10 mmol·L⁻¹) was monitored, and the internal mechanism of the relationship between the forms of energy and the removal of sulfur pollution was analyzed. After the 20-day exposure experiment, the growth and nutrient absorption capacity were significantly inhibited, and this inhibition proved to be concentration-dependent. In addition, high concentrations (4 and 10 mmol·L⁻¹) of NaHSO₃ might affect photosynthesis by disrupting cell membrane systems as it may interfere with membrane proteins and lipids and thus alter membrane integrity. Therefore, the cellular metabolic energy was increased and the sulfur absorption by *I. pseudocorus* was promoted under the low concentration (0.5 mmol/L⁻¹) compared with the control, the role of NaHSO₃ in promoting the growth of *I. pseudocorus* is much greater than its toxic effect under low concentrations. Under the hydroponic culture which contained 0.5 mmol·L⁻¹ of NaHSO₃, *I. pseudocorus* grew well and absorbed more sulfur. The results can be used as a reference for the cultivation of aquatic plants dealing with sulfur pollution, and dilution strategy can be set up to treat water medium that is seriously polluted with sulfur.

**Keywords:** energy conservation equation; electrophysiological parameters; energy consumption; photosynthesis; sulfur pollution

## 1. Introduction

Many plants are very sensitive to environmental changes. Monitoring environmental changes with plants is one of the hotspots and frontiers of future research [1]. Plants in natural or agricultural environments are exposed to short-term changes in environmental conditions, and the adaptability of plants often depends on their rapid response to these highly variable conditions [2]. There are many different types of signal transduction in plants, among these, the electrical signal is a detectable physical quantity or pulse, such as voltage or current, and information can be transmitted through it [3]. Research on plant electrical signals helps to reveal the essence of information exchange in plant cells and organs [4]. Electrical signals regulate and reflect changes in physiological processes such as photosynthesis, substance transport, growth and metabolism in plants and regulate

plant gene expression to adapt to the external environment [4,5]. Retivin et al. [6] have hypothesized that electrical signals are the mechanism of rapid and nonspecific adaptation to stress sources in higher plants; that is, electrical signals can not only transmit specific information about stimulation types but can also contribute to plant tolerance to the effects of various stress sources. Plants have to undergo various stresses in the environment. Understanding stress signals and responses will help to improve plant stress resistance. Plant stress signals evolve from cell energy perception, so understanding the interaction between the stress signal pathways and the growth and development signal pathways is greatly significant [7].

Plant photosynthesis can reflect the potential of plant productivity, and the morphological changes of plants under adversity can directly reflect the resistance of plants [8]. Plants convert light energy into chemical energy by photosynthesis, supporting all energy metabolism in plants. Energy-supporting processes in plants include growth, substance metabolism, ion absorption, resistance to adversity and so on. The cellular metabolic energy of plant leaves is used as the evaluation index of basic plant metabolism. According to the energy conservation law, it can be roughly concluded that the energy consumed by plants to resist adversity under different environmental conditions is equal to the difference between the energy produced by photosynthesis and growth energy consumption and the cellular metabolic energy in plants (Figure 1). The energy required for plant growth and development is called the metabolic energy of plant cells [9]. Metabolic energy can be directly utilized by cell metabolism, and it is also an energy form used by organisms to build themselves and maintain life activities. The process of plant growth and development is supported by the cellular metabolism of plants [10], including physiological and biochemical processes in plants, such as water metabolism, the synthesis and transformation of organic compounds and the assimilation and utilization of inorganic compounds [11].
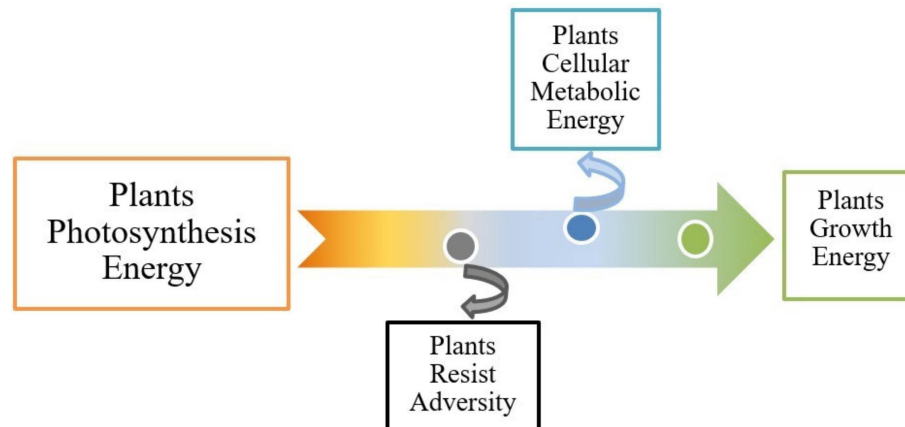


**Figure 1.** Energy consumed by plants according to the energy conservation law.

$SO_2$ is a common atmospheric pollutant, one of the main components of acid rain, that is also widely distributed worldwide. Due to the different resistances of different organisms to $SO_2$ and its derivatives, some sensitive species will disappear, the structure and function of the ecosystem will be affected [12]. Sulfur dioxide is easily dissolved in water to produce sulfuric acid [13]. Under physiological conditions (pH 7.4 and 37 °C), the mixture of sulfite ions ($SO_3^{2-}$) and bisulfite anions ($HSO_3^-$) dominates, and acidification will release sulfur dioxide vapor. Sulfite, bisulfite and metabisulfite are produced in alkali conditions [14], but they are all tetravalent sulfur ($S^{4+}$) substances at different pH values [15]. Plants absorb sulfur dioxide in the air then convert it into sulfate and sulfite in cells. The membrane of mesophyll cells has strictly selective permeability to various ions. When plant leaves are stimulated by the external environment, the permeability of the cytomembrane changes immediately. Leaf resistance (R), impedance (Z) and capacitance (C) are related to cell membrane permeability, ion concentration and cell turgor pressure. These changes can be

reflected by electrical parameters. Studies have shown that the toxicity of $SO_2$ to plants is mainly attributed to the highly active intermediate bisulfite [16]. $NaHSO_3$ ($NaHSO_3$) is one of the most commonly used sulfites. Sulfite in plants can be reduced to sulfide by sulfite reductase or oxidized to sulfate by sulfite oxidase [17]. Low-concentration bisulfite can be used as a photosynthetic accelerator in agricultural production [18]. It has been reported that sulfite ($Na_2SO_3$) and bisulfite ($NaHSO_3$) are sprayed on plant leaves to simulate the $SO_2$ environment. When studying its physiological growth characteristics, it is found that low-concentration treatment can promote the photosynthesis and growth of plants [19]. Previous studies have also proved that it is feasible to enhance photobiological $H_2$ production by decreasing the $O_2$ content in *Anabaena* 7120 cells with $NaHSO_3$ treatment [20]. However, the bisulfite compounds are inhibitors of photosynthetic $CO_2$ fixation, ATP formation in photosynthesis and respiration, $H^+$ fluxes and of $Cl^-$ transport at cell membranes; they may act by way of effects on photosynthetic $CO_2$ fixation or on the ionic relations of the guard cells [21]. The severe damage appeared in the chloroplast of *Pinus massoniana* by the action of simulated $SO_2$, which led to the swelling or disorder of chloroplast and thylakoid [22]. Diversely, toxicity tests showed that situations with an overfeed of sodium thiosulfate or sodium bisulfite can depress pH and dissolve oxygen, causing the mortality of fish [23]. In addition, some studies have shown that $NaHSO_3$, a derivative of $SO_2$ in living organisms, can induce chromosome aberrations in mammalian cells [24], cause an increase in the sister chromatid exchange (SCE) and micronucleus (MN) rate of human lymphocytes in a dose-dependent manner and cause a delay in mitosis and a decrease in the mitotic index [25].

The impact of $NaHSO_3$ on plants and animals has two sides, and its widespread use in agriculture as a growth promoter is bound to cause some environmental pollution. However, there is a lack of systematic and in-depth research on the toxicity mechanism or promoting effect of the $NaHSO_3$ that is discharged into the environment onto animals and plants. Current studies on $NaHSO_3$ focus on the effects it has on photosynthesis but have not paid attention to the accumulation of S element, and there are few studies on aquatic plants. The impact of polluted water sources on the aquatic environment can be evaluated by ecotoxicological tests, and various studies conducted in many countries worldwide have confirmed the importance of applying ecotoxicological tests in practice [26], such as the application of the highly sensitive aquatic biota *Chlorella vulgaris* to the assessment of biological toxicity in river water [27], so the effects of polluted aquatic environments on plant growth can be better characterized by ecotoxicology tests. *Iris pseudocorus* L. is a tall perennial emergent plant and a common plant in ecological landscape construction, often used to remove water pollutants, but its response mechanism to sulfur pollution in water condition is still not clear. In this study, $NaHSO_3$ was used as the sulfur pollution source in water, the response of *I. pseudocorus* to the water environment was monitored. To explore the effect of the concentration range of $NaHSO_3$ on plant growth, the cellular metabolic energy and photosynthesis for toxic or promoting effects, the growth of *I. pseudocorus* and the internal mechanism of the relationship between cellular metabolic energy, photosynthesis and growth under different concentrations of $NaHSO_3$ were investigated, in order to provide a basis for determining the best culture conditions for aquatic plants subjected to bisulfite pollution.

## 2. Materials and Methods

### 2.1. Experimental Materials and Treatment

The *I. pseudocorus* seedlings used in this experiment were purchased from a hydrophyte center in Jiangsu, China. Before the experiment, the *I. pseudocorus* seedlings were precultured in 1/2 Hoagland's solution for 30 days, and the plants with good uniform growth were selected for the experiment.

The experiment was conducted using a hydroponic system with standard Hoagland's solution. The treatment was performed in 10 L buckets with $NaHSO_3$ concentrations of 0 (control), 0.5, 2.0, 4.0 and 10.0 mmol·L$^{-1}$ (hereinafter referred to as $T_0$, $T_{0.5}$, $T_{2.0}$, $T_{4.0}$ and

$T_{10.0}$). Three replicates per group and 7 seedlings per bucket were prepared to ensure the consistency of the individuals. $NaHSO_3$ was dissolved in the liquid nutrient solution, and the volume was fixed at 10 L. During the 20-day experimental period, the nutrient solutions were aerated for half an hour per day to prevent rot development. In addition, the standard Hoagland's solution was replaced once on the 10th day to ensure that the nutrients met the needs of plants and that the nutrient contents for different groups of plants were consistent. The nutrient content was calculated based on the total amount.

### 2.2. Measurement of Growth Index

During the 20-day experiment period, the changes in plant leaf number (the total leaf number of 5 plants in each treatment, taking the average value) and total tiller number were recorded, and the total fresh weight of the treated plants was weighed with an analytical balance (ML503, Mettler Toledo Instrument Co., Ltd., Shanghai, China) every 10 days.

### 2.3. Measurement of Photosynthetic Parameters

The photosynthetic parameters measurement was conducted with a portable Li-6400XT photosynthetic measurement system (Li-COR Inc., Lincoln, NE, USA). The second fully expanded leaf of *I. pseudocorus* plants was selected for measurement on sunny days. The photosynthetic parameters were measured at 9:30–11:30 a.m. on day 0 and on the 10th and 20th day. Using a natural light source for measurement, the leaf temperature was $29 \pm 2$ °C, and the flow rate was set to 500 $\mu mol \cdot s^{-1}$. The net photosynthetic rate ($P_N$), stomatal conductance (gs), intercellular $CO_2$ concentration (Ci) and transpiration rate (E) were recorded.

### 2.4. Measurement of Electrophysiological Parameters and Calculation of Cellular Metabolic Energy

The electrophysiological parameters were measured by a HIOKI 3532-50 LCR tester made in Japan according to Wu et al. [28]. The measurement was performed on day 0, 10 and 20 during the experiment. The second leaf of *I. pseudocorus* was randomly selected and kept wet with distilled water for 30 min. Then, the water on the leaf surface was sucked up, and the leaf was immediately clamped between the parallel electrode plates of the measuring device. The diameter of the electrode plate was 10 mm, the measuring voltage was set to 1.5 V and the measuring frequency to 3000 Hz, changing the pressure of the device by adding the number of iron blocks with a known mass of 0.1 kg (in Newton, N), the physiological capacitance, resistance and impedance of plant leaves under different clamping forces were simultaneously measured in parallel mode (Figure 2).
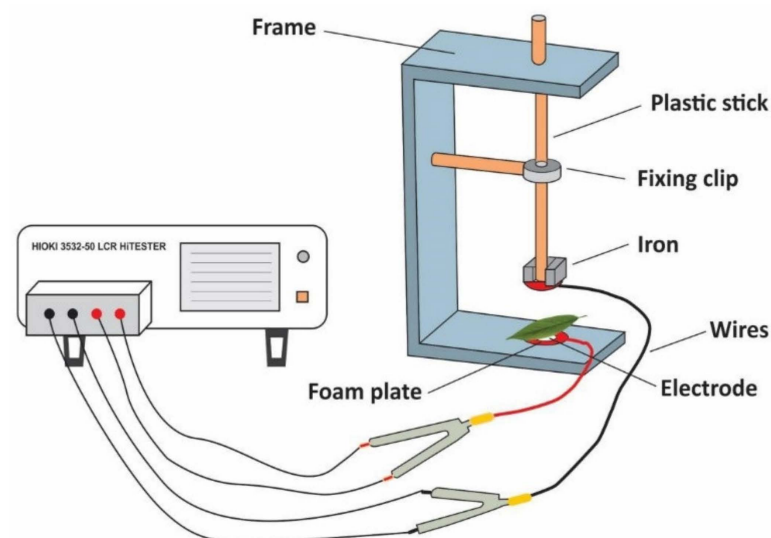


**Figure 2.** Representation of the parallel-plate capacitor attached to the LCR tester [29].

The Gibbs free energy equation is expressed as $\Delta G = \Delta H + PV$, plant cells can be regarded as spherical capacitors, and its energy formula is expressed as $W = \frac{1}{2}U^2 Cp$. $W$ is the energy of the capacitor, equal to the work done by the Gibbs free energy, that is $W = \Delta G$; $\Delta H$ is the internal energy of the system (plant leaf system composed of cells), $P$ is the pressure on plant cells, $V$ is the volume of plant cells, $U$ is the test voltage and $Cp$ is the physiological capacitance of plant leaves; The pressure $P$ on plant cells can be calculated by the pressure formula: $P = \frac{F}{S}$, where $F$ is the clamping force and $S$ is the effective area under the action of the polar plate; Variation model of physiological capacitance $Cp$ of plant leaves with clamping force $F$:

$$Cp = \frac{2\Delta H}{U^2} + \frac{2V}{S \cdot U^2}F \tag{1}$$

Assuming that $d$ represents the specific effective thickness of plant leaves, then $d = \frac{V}{S}$; Formula (1) is deformable to:

$$Cp = \frac{2\Delta H}{U^2} + \frac{2d}{U^2}F \tag{2}$$

Keeping $x_0 = \frac{2\Delta H}{U^2}$, $h = \frac{2d}{U^2}$, Formula (2) can be deformed as follows:

$$Cp = x_0 + hF \tag{3}$$

Formula (3) is a linear model, and $x_0$ and $h$ are model parameters. As $h = \frac{2d}{U^2}$, $d = \frac{U^2 h}{2}$.

Because the resistive current is caused by ion transfer, it is determined by the permeability of the membrane to various ions and the existence of a large number of permeable ions. External excitation changes the permeability of ions and affects the concentration of internal and external ions. The concentration difference of internal and external ions obeys the Nernst equation, and the physiological resistance is inversely proportional to the electrical conductivity, while the electrical conductivity is directly proportional to the ion concentration in cells. Therefore, the relationship between the physiological resistance of cells and external excitation can be deduced.

Under different clamping forces, the permeability of different plant cell membranes changes differently, so their physiological resistance is different.

The expression of the Nernst equation is shown in Formula (4):

$$E - E^0 = \frac{R_0 \cdot T}{n_R \cdot F_0} \ln \frac{C_i}{C_o} \tag{4}$$

where $E$ is the electromotive force; $E^0$ is the standard electromotive force; $R_0$ is the ideal gas constant, equal to $8.314570$ J·K$^{-1}$·mol$^{-1}$, $T$ is the temperature, unit is K; $C_i$ is the permeable ion concentration inside the cytomembrane in response to physiological resistance, $C_o$ is the permeable ion concentration outside the cytomembrane in response to physiological resistance, the total amount of permeable ions inside and outside the membrane in response to physiological resistance $C_T = C_i + C_o$, $F_0$ is the Faraday constant, equal to 96,485 C·mol$^{-1}$; $n_R$ is the number of permeable ion transfers in response to physiological resistance, unit is mol.

The internal energy of electromotive force $E$ can be converted into work done under pressure, which is directly proportional to $P\,V$, $P\,V = a\,E$, that is:

$$P\,V = a\,E = a\,E^0 + \frac{a\,R_0 \cdot T}{n_R \cdot F_0} \ln \frac{C_i}{C_o} \tag{5}$$

where $P$ is the pressure on plant cells, $a$ is the energy coefficient of electromotive force conversion and $V$ is the volume of plant cell.

The pressure $P$ on plant cells can be derived from the pressure formula: $P = \frac{F}{S}$, where $F$ is the clamping force and $S$ is the effective area under the action of the polar plate.

In mesophyll cells, vacuoles and cytoplasm occupy most of the space in the cell. For mesophyll cells, the sum of $C_o$ and $C_i$ is a constant, which is equal to the total amount of

permeable ions $C_T$ in response to physiological resistance inside and outside the membrane. $C_i$ is directly proportional to the conductivity, and the conductivity is the reciprocal of resistance **R**. Therefore, $\frac{C_i}{C_o}$ can be expressed as $\frac{C_i}{C_o} = \frac{\frac{f_0}{R}}{C_T - \frac{f_0}{R}} = \frac{f_0}{C_T R - f_0}$, where **R** is the resistance and $f_0$ is the proportional coefficient of the transformation between the permeable ion concentration $C_i$ in the cell membrane in response to the physiological resistance and the resistance. Therefore, (5) can be rewritten as:

$$\frac{V}{S}F = a\,E^0 - \frac{a\,R_0{\cdot}T}{n_R{\cdot}F_0}\ln\frac{C_T{\cdot}R - f_0}{f_0} \tag{6}$$

Formula (6) can be rewritten as:

$$\frac{a\,R_0{\cdot}T}{n_R{\cdot}F_0}\ln\frac{C_T{\cdot}R - f_0}{f_0} = a\,E^0 - \frac{V}{S}F \tag{7}$$

Taking the logarithm on both sides of Formula (7), we obtain:

$$\ln\frac{C_T{\cdot}R - f_0}{f_0} = \frac{n_R{\cdot}F_0{\cdot}E^0}{R_0{\cdot}T} - \frac{V{\cdot}n_R{\cdot}F_0}{S\,a\,R_0{\cdot}T}F \tag{8}$$

Order $\alpha = \frac{n_R{\cdot}F_0{\cdot}E^0}{R_0{\cdot}T}$, $\beta = \frac{V{\cdot}n_R{\cdot}F_0}{S\,a\,R_0{\cdot}T}$; then, Equation (8) can be deformed as follows:

$$\ln\frac{C_T{\cdot}R - f_0}{f_0} = \alpha - \beta F \tag{9}$$

Taking the index on both sides of Formula (9), it can become:

$$\frac{C_T{\cdot}R - f_0}{f_0} = e^{\alpha}e^{-\beta F} \tag{10}$$

Further deformation can result in:

$$R = \frac{f_0}{C_T} + \frac{f_0}{C_T}e^{\alpha}e^{-\beta F} \tag{11}$$

In Equation (10), $R$ is the physiological resistance, and because $d = \frac{V}{S}$, $\beta = \frac{V{\cdot}n_R{\cdot}F_0}{S\,a\,R_0{\cdot}T}$ in Equation (9) can be deformed as:

$$\gamma = \frac{d\,n_R.F_0}{a\,R_0.T} \tag{12}$$

Further deformed to $R$:

$$R = \frac{f_0}{C_T} + \frac{f_0}{C_T}e^{\alpha}e^{-\gamma F} \tag{13}$$

For the same leaf to be tested under the same environment, $d$, $a$, $E^0$, $R_0$, $T$, $n_R$, $F_0$, $C_T$ and $f_0$ in Equations (11) and (12) are fixed values. Keeping $y_0 = \frac{f_0}{C_T}$, $k_1 = \frac{f_0}{C_T}e^{\alpha}$, $b_1 = -\gamma$. Therefore, Equation (13) can be deformed as:

$$R = y_0 + k_1\,e^{-b_1 F} \tag{14}$$

In Formula (14), $y_0$, $k_1$ and $b_1$ are the parameters of the model. Thus, the unit metabolic energy of plant leaf cells is based on physiological resistance $\Delta G_{R-E} = \frac{a\,E^0}{d} = \frac{\ln k_1 - \ln y_0}{b_1}$. Metabolic energy of plant leaf cells based on physiological resistance $\Delta G_R = \Delta G_{R-E}{\cdot}\,d$.

Similarly, the model of physiological impedance $Z$ of plant leaves varying with clamping force can be constructed as follows:

$$Z = p_0 + k_2\,e^{-b_2 F} \tag{15}$$

In Formula (15), $p_0$, $k_2$ and $b_2$ are the parameters of the model. Therefore, the unit metabolic energy of plant leaf cells is based on physiological impedance $\Delta G_{Z-E} = \frac{a\,E^0}{d} = \frac{\ln k_2 - \ln p_0}{b_2}$. The metabolic energy of plant leaf cells is based on physiological impedance $\Delta G_Z = \Delta G_{Z-E} \cdot d$.

In this paper, the cellular metabolic energy $\Delta G_B$ is the mean value of $\Delta G_R$, based on physiological resistance, and $\Delta G_Z$, based on physiological impedance.

The critical steps in calculating cellular metabolic energy are shown in Figure 3.
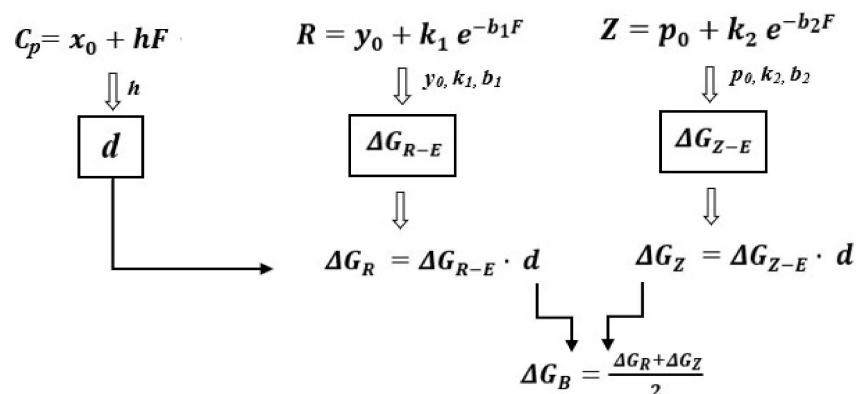


**Figure 3.** Critical steps in calculating cellular metabolic energy.

*2.5. Determination of the pH Value of the Tested Environment and Kinetic Model of Sulfur Absorption*

In the 20-day experiment, the pH value changes of the Hoagland's solution containing NaHSO$_3$ were detected and recorded from day 0 to the 10th day using a pH meter (PHSJ-3F, INESA Scientific Instrument Co., Ltd., Shanghai, China). A 20 mL water sample was taken every day in each treatment group to measure the total sulfur content of the treated water samples. The measurement refers to the method of Zhang et al. [30]. The steps are as follows: take an appropriate amount of water sample and add distilled water to 50 mL, add the supernatant of calcium oxide to the water sample, then add the potassium permanganate solution, adjust the solution with sodium hydroxide until the solution is slightly alkaline, then heat it on an electric heating plate and keep it slightly boiling for 15 min. If the color purple disappears during the heating process, add a small amount of potassium permanganate to maintain light purple. Replenish the volume of water sample with distilled water, add nitric acid solution to the water sample, keep it in a slightly boiling state for 10 min. Replenish the volume of water sample with distilled water, add hydrochloric acid solution to the water sample and heat it for 5 min, remove the water sample, use the Barium Chromate Spectrophotometry method to measure the sulfate in the water sample, then convert it into sulfur content. It is generally believed that the absorption of inorganic ions by plants is an active process. The ion absorption kinetic model is constructed based on the measurement of total sulfur content in water samples. The method is as follows:

It is described quantitatively in the Michaelis–Menten equation shown in formula (16) or the modified form shown in formula (17).

$$V = \frac{V_{max}}{K_m + C} \tag{16}$$

$$V_{in} = \frac{V_{max}(C - C_{min})}{K_m + (C - C_{min})} \tag{17}$$

In the formula, $V$ is the ion absorption rate (mg·L$^{-1}$·D$^{-1}$); $V_{max}$ is the maximum absorption rate (mg·L$^{-1}$·D$^{-1}$); $C$ is the ion concentration in extracellular solution (mg·L$^{-1}$); $K_m$ is the Michaelis constant (mg·L$^{-1}$); $V_{in}$ is the net absorption rate; $C_{min}$ is the critical concentration or balanced concentration of the ion in extracellular solution (mg·L$^{-1}$), that is, the ion concentration in extracellular solution when $V_{in} = 0$. The smaller its value is, the

stronger the ability of plants to absorb nutrients at low concentrations. $V_{max}$, $K_m$ and $C_{min}$ are three parameters characterizing the kinetic characteristics of plant nutrient absorption. The method is as follows [31–34]:

First, the ion consumption curve is drawn according to the concentration of absorption solution and the absorption time, and then the ion consumption curve equation is obtained. The common ion consumption curve equation is a unary quadratic polynomial:

$$C = m + nT + pT^2 \qquad (18)$$

Here, $C$ is the concentration of absorbed ions, $T$ is the absorption time, and $m$, $n$ and $p$ are equation coefficients.

Taking the first negative derivative from Equation (18), the ion consumption rate equation is obtained:

$$C' = -n - 2pT \qquad (19)$$

Formula (19) is treated as follows: let $T \to 0$; then, $C' = -n$, which is the maximum change rate of concentration. Afterwards, according to the water sample dilution concentration $N$ ($N = 1/5$), the maximum absorption rate $V_{max}$ (specific maximum absorption rate) of *I. pseudocorus* per day was calculated, i.e.,

$$V_{max} = -n/N \qquad (20)$$

Put $C' = -n/2$ into Equation (19) to deduce $T$, and then put $T$ back into Formula (18) to deduce $C$, that is, the value of $K_m$.

Let $C' = 0$, obtain the time $T$ when the absorption rate is 0, replace $T$ back into Formula (18), and calculate the value of equilibrium concentration $C_{min}$.

To better evaluate and compare the nutrient absorption rate of plants, parameter $\alpha$ based on two basic kinetic parameters, $V_{max}$ and $K_m$, was introduced.

$$\alpha = V_{max}/K_m \qquad (21)$$

$K_m$ is usually used as the evaluation index of plant affinity for nutrient ions, but when $V_{max}$ and $K_m$ change cooperatively, $K_m$ cannot well reflect the actual affinity, and the ratio of $V_{max}$ and $K_m$ is $\alpha$, which is a better affinity evaluation index [35,36]. The higher the value of $\alpha$, the stronger the affinity, and the faster the rate of ions entering the plant.

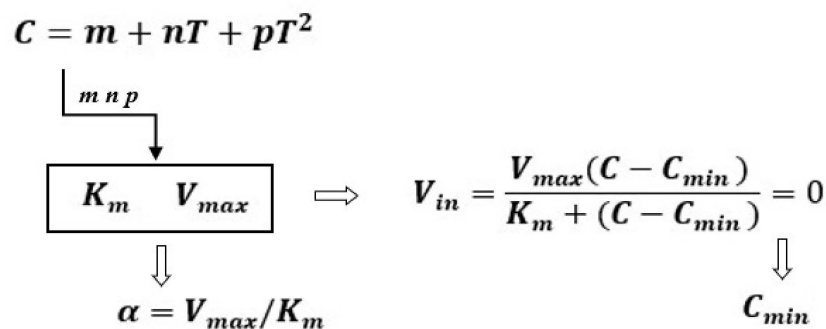The critical steps in calculating the kinetic model of sulfur absorption are shown in Figure 4.



**Figure 4.** Critical steps in calculating the kinetic model of sulfur absorption.

### 2.6. Normalization of Experimental Data

Although we can use different physiological indices to characterize the productivity, resistance and growth efficiency of *I. pseudocorus*, there are obvious differences between different physiological indices, such as units, dimensions and thresholds. Therefore, the net photosynthetic rate ($P_N$), the cellular metabolic energy of plant leaf ($\Delta G_B$) and the fresh weight of plants all need to be normalized in a unified mode. $W_{PN}$ represents the

energy produced by photosynthesis, $\Delta G_B$ represents the cellular metabolic energy, $\Delta W_G$ represents the energy consumption for plant growth and $W_S$ represents the energy required to resist adversity. $\Delta W_G$ is expressed as the growth rate of plant fresh weight, representing the energy required for plant growth and development:

$$\Delta W_G = W_i / W_0 - 1 \tag{22}$$

where $W_i$ is the fresh weight of each treatment and control group on the 10th and 20th days, and $W_0$ is the fresh weight of each treatment and control group within 2 h.

According to the law of conservation of energy, the equation is constructed:

$$W_{PN} = \Delta G_B + \Delta W_G + W_S \tag{23}$$

The measured data were normalized to better compare the plant growth conditions characterized by different physiological indices. The method is:

$$N = N_i / N_{CK} \tag{24}$$

$N$ is the value after normalization. If the $P_N$ is normalized, $N$ represents $N_{PN}$, $N_i$ represents the $P_N$ of each effective sample, and $N_{CK}$ represents the $P_N$ of the control group in the same period of each effective sample. If the $\Delta G_B$ is normalized, and $N$ stands for $N_{\Delta G_B}$ and $N_i$ represents the $\Delta G_B$ of each effective sample, $N_{CK}$ represents the $\Delta G_B$ in the control group in the same period of each effective sample. By analogy, the $\Delta W_G$ can be normalized.

According to Formula (23), after normalization, the energy required to resist adversity $N_{WS}$ is as follows:

$$N_{WS} = N_{PN} - N_{\Delta G_B} - N_{\Delta W_G} \tag{25}$$

After normalization, the $N_{WS}$ value of the control group was $-1$ on the 10th and 20th days. To facilitate comparison, $N_{WS1}$, based on the parameter $N_{WS}$, was introduced,

$$N_{WS1} = N_{WS} + 1 \tag{26}$$

Compared with $N_{WS}$, $N_{WS1}$ can more intuitively evaluate and compare the additional energy consumed by plants in the environment.

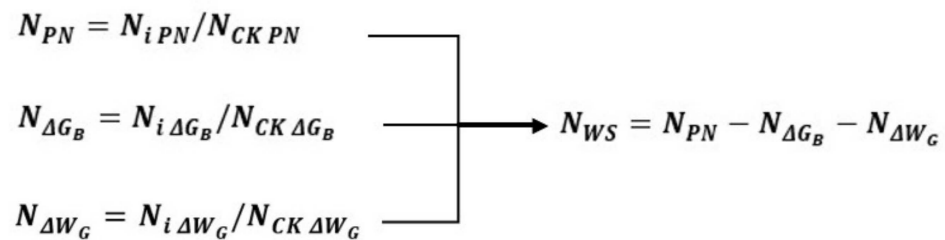The critical steps in normalization are shown in Figure 5.



$$N_{PN} = N_{i\,PN} / N_{CK\,PN}$$

$$N_{\Delta G_B} = N_{i\,\Delta G_B} / N_{CK\,\Delta G_B} \longrightarrow N_{WS} = N_{PN} - N_{\Delta G_B} - N_{\Delta W_G}$$

$$N_{\Delta W_G} = N_{i\,\Delta W_G} / N_{CK\,\Delta W_G}$$

**Figure 5.** Critical steps in normalization.

*2.7. Statistical Analysis*

All experiments were conducted at least three times. The data are expressed as the means $\pm$ SE. The results are calculated and plotted with Origin 9.0. IBM SPSS Statistics version 23.0 was used for one-way ANOVA to compare the differences among different treatments. The significance level was $p < 0.05$.

## 3. Results

*3.1. Effects of Different Treatments on the Growth of I. pseudocorus*

The growth of *I. pseudocorus* after the 20-day treatment is shown in Figure 6. The fresh weight of *I. pseudocorus* was related to plant activity of life, and adverse environmental

factors can inhibit the increase in fresh weight. Table 1 shows the effect of different $NaHSO_3$ treatments on the fresh weight of *I. pseudocorus* over time.



**Figure 6.** The Growth of *I. pseudocorus* after 20-day treatment.

**Table 1.** Variations in the total fresh weight of *I. pseudocorus* over time under different $NaHSO_3$ treatments (unit: g).

| | $T_0$ | $T_{0.5}$ | $T_{2.0}$ | $T_{4.0}$ | $T_{10.0}$ |
|---|---|---|---|---|---|
| 0 d | $494.60 \pm 1.19$ [aw] | $497.50 \pm 1.89$ [aw] | $494.13 \pm 1.60$ [aw] | $494.80 \pm 1.39$ [au] | $496.03 \pm 1.12$ [au] |
| 10 d | $586.17 \pm 1.59$ [av] | $577.83 \pm 0.73$ [bv] | $556.50 \pm 0.51$ [cv] | $425.57 \pm 0.50$ [dv] | $352.53 \pm 0.74$ [ev] |
| 20 d | $796.50 \pm 1.31$ [au] | $765.17 \pm 0.73$ [bu] | $646.77 \pm 0.59$ [cu] | $317.93 \pm 0.71$ [dw] | $240.70 \pm 0.85$ [ew] |

Note: Compared with the same measurement time, a, b, c, etc. indicates that the means $\pm$ SE of total fresh weight in different treatment groups is significantly different when $p \leq 0.05$; Compared with the same treatment group, u, v, w indicates that the means $\pm$SE of the total fresh weight at different treatment time was significantly different when $p \leq 0.05$.

In the experimental period, the plants showed a significantly lower fresh weight in all treatment groups compared with that of the control. With increasing treatment time, the fresh weight increased significantly at $T_{0.5}$ and $T_{2.0}$ treatment levels, while the fresh weight decreased significantly at $T_{4.0}$ and $T_{10.0}$ treatment levels, and the higher the treatment concentration, the lower the fresh weight.

With increasing concentrations of $NaHSO_3$, the fresh weight of *I. pseudocorus* exhibited a sharp decrease. Under severe stress, shrinkage and dehydration occurred in the plants, and the plants dried up and died in the latter period of the experiment.

The inhibition on leaf growth was clearly observed in the presence of $NaHSO_3$ (Table 2). In the absence of $NaHSO_3$, the number of plant leaves in the control group remained stable. With increasing concentration of $NaHSO_3$, the number of plant leaves showed no significant difference at $T_{0.5}$, $T_{2.0}$ levels, but exhibited significant decrease at $T_{4.0}$ and $T_{10.0}$ levels. When the $NaHSO_3$ concentration increased to 4 mmol·$L^{-1}$, dehydration and shrinkage occurred in the leaves on the 10th day from the onset of the treatment, and the time was reduced to 5 days when the bisulfite concentration increased to 10 mmol·$L^{-1}$.

The effect of $NaHSO_3$ on the average tillers of *I. pseudocorus* is shown in Table 3. Plants produce tillers through vegetative propagation, and the number of vegetative tillers can indicate the ability of vegetative propagation [37]. The number of plant tillers under different $NaHSO_3$ treatments was significantly lower than that of the control group. The results indicated that the growth of vegetative tillers tended to decrease when $NaHSO_3$ was

added to the treatment groups. Therefore, NaHSO₃ has inhibitory effects on the growth and development of *I. pseudocorus* leaves and tillers.

**Table 2.** Variations in the average leaf number of *I. pseudocorus* under different NaHSO₃ treatments (unit: piece).

| NaHSO₃ Added (mmol·L⁻¹) | 0 d | 5 d | 10 d | 15 d | 20 d |
|---|---|---|---|---|---|
| 0 | 7.80 ± 0.37 [a] | 10.00 ± 0.45 [a] | 10.60 ± 0.68 [a] | 10.40 ± 0.49 [a] | 10.20 ± 0.80 [a] |
| 0.5 | 7.60 ± 0.60 [a] | 8.60 ± 0.60 [a] | 9.40 ± 0.68 [ab] | 10.00 ± 0.60 [a] | 11.00 ± 0.71 [a] |
| 2.0 | 7.20 ± 0.49 [a] | 9.00 ± 0.45 [a] | 9.80 ± 0.20 [ab] | 10.50 ± 0.63 [a] | 11.60 ± 0.24 [a] |
| 4.0 | 7.40 ± 0.93 [a] | 8.40 ± 0.68 [a] | 8.40 ± 0.98 [b(wi)] | 7.20 ± 0.80 [b(wi)] | 6.40 ± 0.40 [b(wi)] |
| 10.0 | 7.20 ± 0.20 [a] | 6.00 ± 0.32 [b(wi)] | 5.20 ± 0.20 [c(wi)] | 4.40 ± 0.24 [c(wi)] | 3.60 ± 0.24 [c(wi)] |

Note: (wi) represents withering, which means that the plants in that group gradually dried up. Compared with the same measurement time, (a, b, c, etc.) indicates that the mean ± SE of the average number of leaves of *I. pseudocorus* is significantly different when $p \leq 0.05$.

**Table 3.** Variations in average tillers of *I. pseudocorus* under different NaHSO₃ treatments (unit: plant).

| NaHSO₃ Added (mmol·L⁻¹) | 0 d | 5 d | 10 d | 15 d | 20 d |
|---|---|---|---|---|---|
| 0 | 0.000 | 0.000 | 0.000 | 0.429 | 1.000 |
| 0.5 | 0.000 | 0.000 | 0.143 | 0.143 | 0.143 |
| 2.0 | 0.000 | 0.000 | 0.000 | 0.072 | 0.143 |
| 4.0 | 0.000 | 0.000 | 0.143 | 0.214 | 0.429 |
| 10.0 | 0.000 | 0.000 | 0.000 | 0.000 | 0.000 |

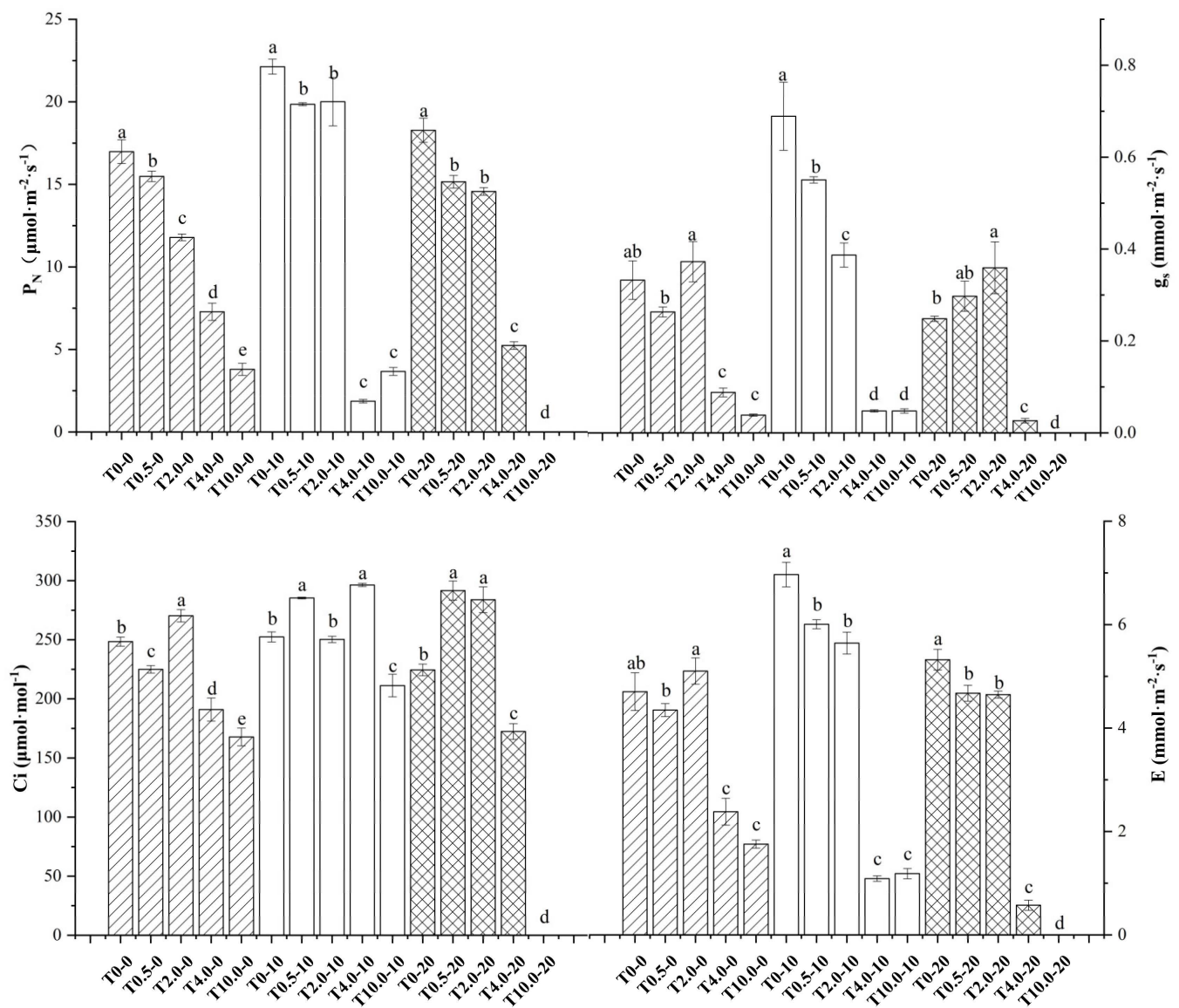*3.2. Effects of Different Concentrations of NaHSO₃ on the Photosynthesis of I. pseudocorus*

The accumulation of plant biomass is closely related to photosynthesis. Figure 7 shows the changes in the photosynthetic characteristics of *I. pseudocorus* under NaHSO₃ treatment. Within 2 h of the treatment, the net photosynthetic rate ($P_N$) significantly decreased with increasing treatment concentration ($p < 0.05$). The stomatal conductance (gs), intercellular $CO_2$ concentration (Ci) and transpiration rate (E) exhibited similar trends with $P_N$, while those in $T_{2.0}$ were higher than those in the other treatment groups.

After 10 days of NaHSO₃ exposure, $P_N$, gs and E in the low-concentration treatment groups of $T_{0.5}$ and $T_{2.0}$ were significantly higher than those in the high-concentration treatment groups of $T_{4.0}$ and $T_{10.0}$ ($p < 0.05$), while $T_0$ was significantly higher than that in the low-concentration treatment groups ($p < 0.05$).

After receiving treatment for 20 days, $P_N$, gs, Ci and E in the low-concentration treatment groups of $T_{0.5}$ and $T_{2.0}$ were significantly higher than those in the high-concentration treatment groups of $T_{4.0}$ and $T_{10.0}$. $P_N$ and E under $T_0$ were significantly higher than those in the low-concentration treatment groups, and gs and Ci under $T_0$ were lower than those in the low-concentration treatment groups.

*3.3. Effects of Different Concentrations of NaHSO₃ on the Cellular Metabolic Energy of I. pseudocorus*

The energy in plants used for growth and development is called cellular metabolic energy [10]. One leaf sample of *I. pseudocorus* at each treatment group was taken as an example. Under each treatment concentration of NaHSO₃ and each treatment time, the fitting curves C-F, R-F and Z-F between the clamping force F on the leaf and the capacitance C, resistance R and impedance Z of the leaf are shown in Figure 8. The correlation coefficient $R^2$ of the fitting equation was greater than 0.9, and the *p* value was less than 0.0001. After receiving treatment for 20 days, the leaves of *I. pseudocorus* under $T_{10.0}$ had completely withered, so there were no electrophysiological parameters in $T_{10.0}$-20.
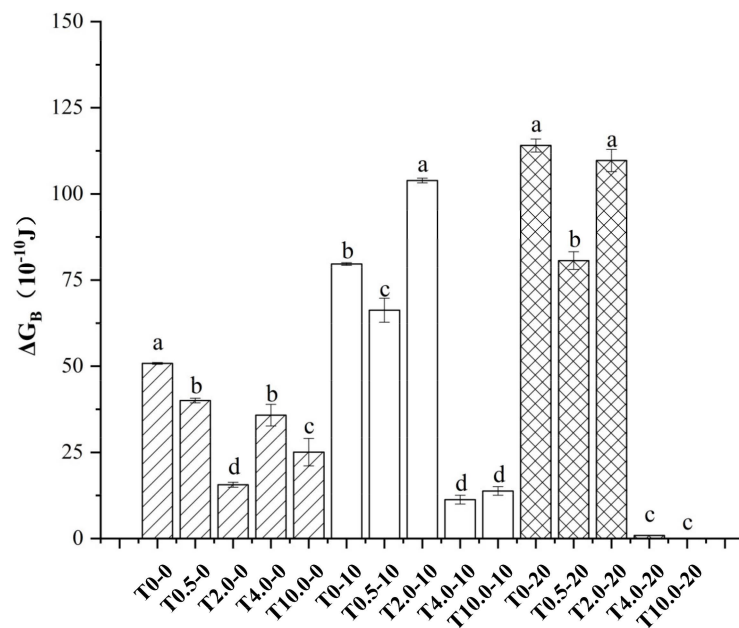
**Figure 7.** Effects of different concentrations of $NaHSO_3$ on the photosynthetic parameters of *I. pseudocorus*. $T_0$-0 indicates the control group before treated, the addition of $NaHSO_3$ was 0 mmol·$L^{-1}$, $T_{0.5}$-0 indicates that the addition of $NaHSO_3$ was 0.5 mmol·$L^{-1}$ and was treated for 2 h, $T_{2.0}$-0 indicates that the addition of $NaHSO_3$ was 2 mmol·$L^{-1}$ and was treated for 2 h, the same below; $T_0$-10 represents the 10th day of the control group, $T_{0.5}$-10 indicates that the addition of $NaHSO_3$ was 0.5 mmol·$L^{-1}$ and was treated for 10 days, $T_{2.0}$-10 indicates that the addition of $NaHSO_3$ was 2 mmol·$L^{-1}$ and treated for 10 days, the same below; $T_0$-20 represents the 20th day of the control group, $T_{0.5}$-20 indicates that the addition of $NaHSO_3$ was 0.5 mmol·$L^{-1}$ and treated for 20 days. In addition, the same is true below. Compared with the same measurement time, (a, b, c, etc.) indicates that the mean ± standard error of photosynthetic parameters of *I. pseudocorus* was significantly different when $p \leq 0.05$.

It can be seen from Figure 9 that cellular metabolic energy under $NaHSO_3$ treatment levels showed significantly lower values than that at $T_0$ level within 2 h of treatment, among which the values at $T_{2.0}$ was significantly lower than that of the other treatment groups. On the 10th day of the treatment, the cellular metabolic energy under the low-concentration treatment groups ($T_0$ and $T_{0.5}$) was significantly higher than that under the high-concentration treatment groups ($T_{4.0}$ and $T_{10.0}$) ($p < 0.05$). The cellular metabolic energy under $T_{2.0}$ was significantly higher than that under the other treatment groups.
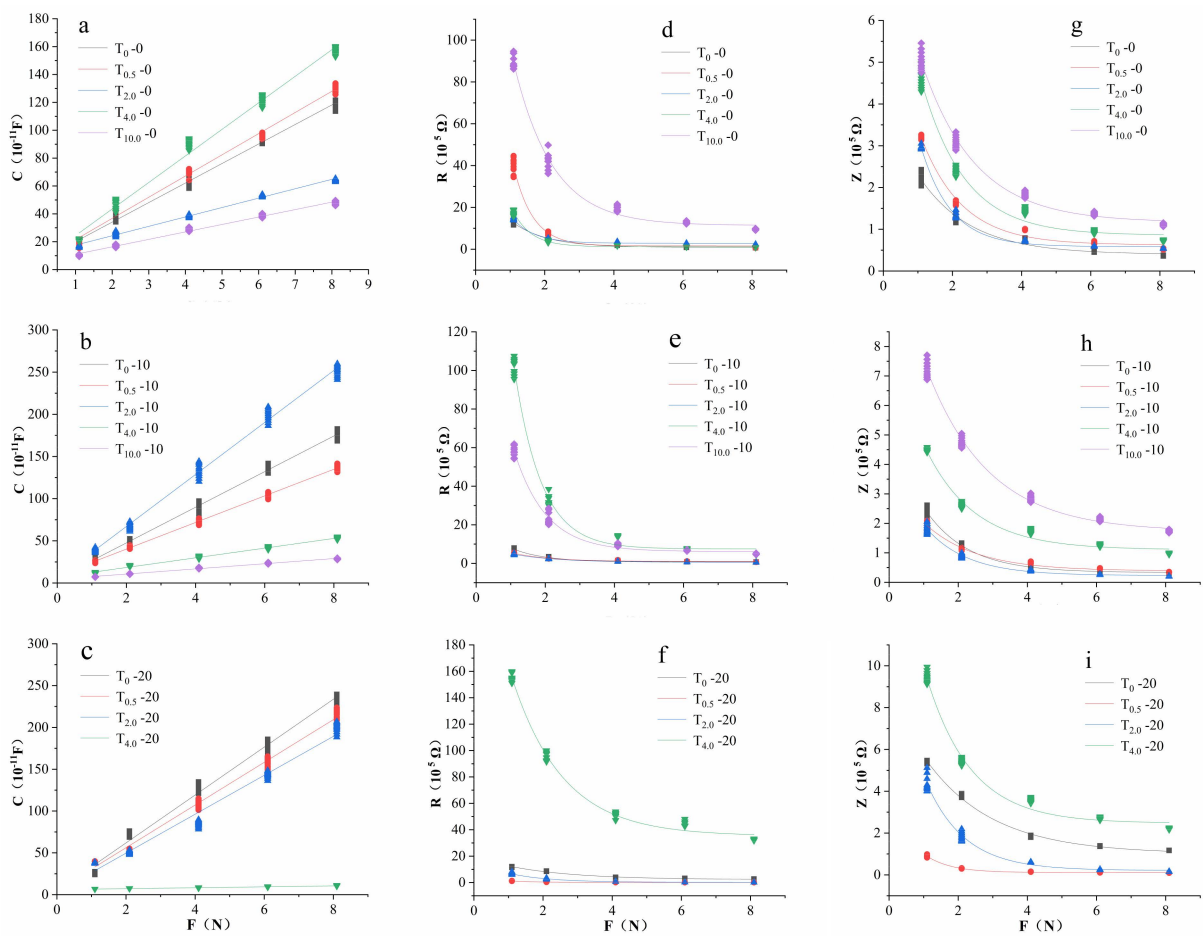
**Figure 8.** Fitting curve of the relationship between C (a, b and c, unit: $10^{-11}$F), R (d, e and f, unit: $10^{5}\Omega$), Z (g, h and i, unit: $10^{5}\Omega$) and clamping force (F, unit: N) of *I. pseudocorus* leaves.



**Figure 9.** Effects of different concentrations of $NaHSO_3$ on the cellular metabolic energy of *I. pseudocorus*. Compared with the same measurement time, (a, b, c, etc.) indicates that the mean $\pm$ SE of the metabolic energy of *I. pseudocorus* is significantly different when $p \leq 0.05$.

After receiving treatment for 20 days, the cellular metabolic energy showed no significant difference between $T_{2.0}$ and $T_0$, and the value at $T_{0.5}$ was significantly lower than those at $T_0$ and $T_{2.0}$. Under the high-concentration treatment groups ($T_{4.0}$ and $T_{10.0}$), the cellular metabolic energy was almost equal to 0.

The results indicate that the plants suffered from stress conditions caused by high concentrations of $NaHSO_3$. In Figure 6, the metabolic energy of plants under the low-concentration treatment groups ($T_{0.5}$, $T_{2.0}$ and $T_0$) progressively increased with increasing treatment time, while the high-concentration treatment groups ($T_{4.0}$ and $T_{10.0}$) decreased gradually. Although the increase of the $NaHSO_3$ concentration could increase the metabolic energy when the $NaHSO_3$ was not higher than 2 mmol·$L^{-1}$, the promoting effect of $NaHSO_3$ on plants was time-limited.

### 3.4. Variations of pH Value in Treatment Solutions

pH is one of the most important conventional indicators to evaluate water quality, as it can affect the growth of aquatic plants. During the exposure experiments, the change in pH of the nutrient solution with different concentrations of $NaHSO_3$ was detected every other day within the first 10 days. The results are shown in Table 4.

**Table 4.** Changes of pH value.

| NaHSO$_3$ Added (mmol·L$^{-1}$) | d 0 | d 2 | d 4 | d 6 | d 8 | d 10 | ΔpH | Means of pH |
|---|---|---|---|---|---|---|---|---|
| 0 | 6.80 ± 0.03 [a] | 6.65 ± 0.05 [a] | 6.60 ± 0.06 [a] | 6.61 ± 0.06 [a] | 6.70 ± 0.03 [a] | 6.60 ± 0.04 [a] | 0.20 | 6.66 |
| 0.5 | 6.71 ± 0.03 [a] | 6.37 ± 0.09 [b] | 6.29 ± 0.03 [b] | 5.89 ± 0.02 [b] | 5.91 ± 0.02 [b] | 6.02 ± 0.01 [b] | 0.69 | 6.20 |
| 2.0 | 5.99 ± 0.08 [b] | 5.32 ± 0.04 [c] | 5.19 ± 0.04 [c] | 4.60 ± 0.01 [c] | 4.41 ± 0.03 [c] | 4.31 ± 0.01 [c] | 1.68 | 4.97 |
| 4.0 | 5.10 ± 0.04 [c] | 4.25 ± 0.03 [d] | 3.65 ± 0.03 [d] | 3.60 ± 0.04 [d] | 3.42 ± 0.04 [d] | 3.33 ± 0.02 [d] | 1.77 | 3.89 |
| 10.0 | 3.21 ± 0.08 [d] | 3.08 ± 0.04 [e] | 3.01 ± 0.02 [e] | 3.01 ± 0.01 [e] | 2.90 ± 0.03 [e] | 2.80 ± 0.03 [e] | 0.41 | 3.00 |

Note: ΔpH = d10–d0. Compared with the same measurement time, (a, b, c, etc.) indicates that the means ± SE of pH values in different Hoagland's solutions were significantly different when $p \leq 0.05$.

The treatment nutrient solution was an $SO_2$-aqueous solution of $NaHSO_3$, with an initial pH value of approximately 6.80 under $T_0$, and the higher the concentration was, the lower the pH value in the treatment nutrient solutions. At 10 mmol·$L^{-1}$, the initial pH value was approximately 3.21. In addition, the pH value decreased over time in the treatment nutrient solutions, while the control group showed a fluctuating trend.

The plants at $T_0$ and $T_{0.5}$ levels grew well in a weakly acidic environment. Although the plants had certain resistance to a stressful environment, as $T_{2.0}$ treatment showed little inhibition on the growth, an acidic environment could also cause adverse effects on the growth of the plants, as plant leaves at $T_{4.0}$ and $T_{10.0}$ levels showed dehydration and shrinkage. These results confirmed the conclusion that high concentrations of $NaHSO_3$ could inhibit the growth of *I. pseudocorus*.

### 3.5. Sulfur Content in Treatment Solutions

$NaHSO_3$ may affect the nutrient absorption capacity of *I. pseudocorus* by affecting the growth and development of the plants, and the total sulfur consumption in treatment solutions was related to the nutrient absorption capacity. The total sulfur consumption curve of *I. pseudocorus* is shown in Figure 10. The total sulfur concentration of $T_0$ level and the low-concentration treatment groups ($T_{0.5}$, $T_{2.0}$) decreased over treatment time, the decrease was severe in the first 4 days, then slowed down to a stable level, indicating that the *I. pseudocorus* absorbed sulfur in the treatment solutions in the process of plant development. The total sulfur concentration under the high-concentration treatment groups ($T_{4.0}$ and $T_{10.0}$) changed little in the 10-day treatment cycle, reflecting that the high-concentration treatment adversely affected the growth of *I. pseudocorus*.
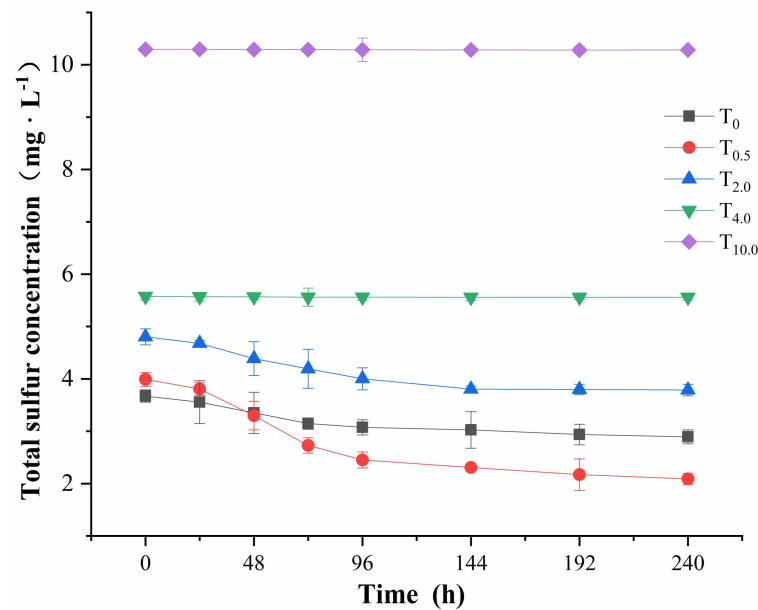
**Figure 10.** Variation in total sulfur content (expressed as total sulfur concentration) with time in Hoagland's solutions with different concentrations of NaHSO$_3$.

When referring to Formula (18), the relationship between the total sulfur concentration and time was analyzed by nonlinear regression analysis (Figure 10), and the fitting equation for the total sulfur consumption curve in Hoagland's solutions with different concentrations of NaHSO$_3$ was obtained, as shown in Table 5. The kinetic parameters for total sulfur absorption were derived from the equation, as shown in Table 6.

**Table 5.** Fitting equations for the relationship between total sulfur concentration (y) and time (x) in Hoagland's solutions.

| Concentrations of NaHSO$_3$ Added (mmol·L$^{-1}$) | Regression Equations | $R^2$ | $p$ |
|---|---|---|---|
| 0 | $y = 0.2737\,x^2 - 4.6279\,x + 88.202$ | 0.972 | <0.001 |
| 0.5 | $y = 0.711\,x^2 - 11.730\,x + 97.935$ | 0.970 | <0.001 |
| 2.0 | $y = 0.393\,x^2 - 6.450\,x + 116.469$ | 0.989 | <0.0001 |
| 4.0 | $y = 0.0082\,x^2 - 0.1189\,x + 133.790$ | 0.977 | <0.0001 |
| 10.0 | $y = 0.0049\,x^2 - 0.0796\,x + 247.121$ | 0.987 | <0.0001 |

**Table 6.** Kinetic parameters for total sulfur absorption in the Hoagland's solutions.

| Concentrations of NaHSO$_3$ Added (mmol·L$^{-1}$) | $V_{max}$ (mg·L$^{-1}$·d$^{-1}$) | $K_m$ (mg·L$^{-1}$) | $C_{min}$ (mg·L$^{-1}$) | $\alpha$ |
|---|---|---|---|---|
| 0 | 22.047 | 74.224 | 69.565 | 0.0594 |
| 0.5 | 58.652 | 61.653 | 49.559 | 0.1903 |
| 2.0 | 32.250 | 96.631 | 90.019 | 0.0667 |
| 4.0 | 0.595 | 133.467 | 133.359 | 0.0009 |
| 10.0 | 0.398 | 246.878 | 246.797 | 0.0003 |

The R$^2$ of each fitting equation ranged from 0.970 to 0.989, $p < 0.001$ (Table 5). Therefore, the change in total sulfur concentration in Hoagland's solution over time at each NaHSO$_3$ treatment group conformed to the univariate quadratic equation, so the estimated kinetic parameters were of high reliability.

The maximum total sulfur absorption rate of *I. pseudocorus* was equal to the product of the absolute value of the coefficient derived from the primary term of the equation and the dilution factor (diluted 5 times); the larger the absolute value was, the larger the maximum absorption rate of total sulfur. The largest absorption rate of sulfur in

*I. pseudocorus* was observed at $T_{0.5}$ level. Compared with the control group ($T_0$), the absolute value of the primary term coefficient decreased, indicating that the absorption rate of sulfur in *I. pseudocorus* decreased with increasing $NaHSO_3$ concentration.

The kinetic parameters $V_{max}$ and $\alpha$ at $T_{0.5}$ level were the largest, while the $K_m$ and $C_{min}$ were the smallest compared with those values under the control and other treatment groups (Table 6), which indicated that 0.5 mmol·$L^{-1}$ $NaHSO_3$ promoted the absorption of sulfur by *I. pseudocorus*, and the promotion effect was the greatest; The kinetic parameters $V_{max}$ and $\alpha$ at $T_{2.0}$ level were higher, but the $K_m$ and $C_{min}$ were lower than the value under the control group, which indicated that 2 mmol·$L^{-1}$ $NaHSO_3$ promoted the absorption of sulfur by *I. pseudocorus*. At $T_{4.0}$ and $T_{10.0}$ levels, the kinetic parameters $V_{max}$ and $\alpha$ were lower, but the $K_m$ and $C_{min}$ were higher compared with that under the control group, this showed that the 4 mmol·$L^{-1}$ and 10 mmol·$L^{-1}$ $NaHSO_3$ inhibited the absorption of sulfur by *I. pseudocorus*, and the higher the concentration of $NaHSO_3$, the greater the inhibition effect. Moreover, the sulfur absorption capacity and growth of *I. pseudocorus* decreased with increasing $NaHSO_3$ concentration.

### 3.6. Results of Data Normalization

The data were normalized using methods described in 2.6. The comprehensive analyses and inferences on growth inhibition, photosynthesis, cellular metabolic energy and nutrient absorption show that $NaHSO_3$ could significantly inhibit the growth and development of *I. pseudocorus*, as shown in Table 7.

**Table 7.** Normalized results of energy indices and $\Delta W_G$ of *I. pseudocorus* under different $NaHSO_3$ treatments.

| Treatment Time | $NaHSO_3$ Added (mmol·$L^{-1}$) | $\Delta W_G$ | $NP_N$ | $N\Delta G_B$ | $N\Delta W_G$ | $NP_N$-$N\Delta G_B$ | NWS | NWS1 |
|---|---|---|---|---|---|---|---|---|
| 2 h | 0 | 0 | 1.000 | 1.000 | 0 | 0 | 0 | |
| 2 h | 0.5 | 0 | 0.912 | 0.788 | 0 | 0.123 | 0.123 | |
| 2 h | 2.0 | 0 | 0.694 | 0.308 | 0 | 0.387 | 0.387 | |
| 2 h | 4.0 | 0 | 0.429 | 0.705 | 0 | −0.276 | −0.276 | |
| 2 h | 10.0 | 0 | 0.224 | 0.494 | 0 | −0.270 | −0.270 | |
| 10 d | 0 | 0.185 | 1.000 | 1.000 | 1.000 | 0 | −1 | 0 |
| 10 d | 0.5 | 0.162 | 0.897 | 0.832 | 0.872 | 0.066 | −0.807 | 0.193 |
| 10 d | 2.0 | 0.126 | 0.904 | 1.304 | 0.682 | −0.400 | −1.082 | −0.082 |
| 10 d | 4.0 | −0.140 | 0.084 | 0.142 | −0.756 | −0.057 | 0.699 | 1.699 |
| 10 d | 10.0 | −0.289 | 0.166 | 0.173 | −1.563 | −0.008 | 1.555 | 2.555 |
| 20 d | 0 | 0.610 | 1.000 | 1.000 | 1.000 | 0 | −1 | 0 |
| 20 d | 0.5 | 0.538 | 0.829 | 0.707 | 0.881 | 0.122 | −0.759 | 0.241 |
| 20 d | 2.0 | 0.309 | 0.797 | 0.962 | 0.506 | −0.165 | −0.671 | 0.329 |
| 20 d | 4.0 | −0.358 | 0.287 | 0.008 | −0.586 | 0.279 | 0.864 | 1.864 |
| 20 d | 10.0 | −0.515 | 0.000 | 0.000 | −0.843 | 0 | 0.843 | 1.843 |

Within 2 h of the treatment, Table 7 shows that the net photosynthetic rate of the high-concentration treatment groups was less than 50% of that of the control group, while that of the low-concentration treatment groups was more than 50%, reflecting that the short-term inhibitory effect of the high-concentration treatment on *I. pseudocorus* was stronger than that of the low-concentration treatment groups. The cellular metabolic energy of the treatment groups all decreased, and the greatest reduction was observed at $T_{2.0}$ level, which was only 30.75% of that under the control group. From the value of $N_{WS}$, plants at $T_{2.0}$ level showed the most energy consumption for adversity resistance among all treatment groups, plants in the two low-concentration treatment groups showed higher energy consumption for adversity resistance than those in the control group, while the plants in the two high-concentration treatment groups showed lower energy consumption for adversity resistance than those in the control group.

After receiving treatment for 10 days, the net photosynthetic rate of the low-concentration treatment groups was close to 90% of that of the control group, while the two high-

concentration treatment groups showed less than 20% of that of the control group. The cellular metabolic energy at $T_{2.0}$ level was 130.41% of that of the control group, the value at $T_{0.5}$ level was 83.17% of that of the control group, while high-concentration treatment groups showed less than 20% of that of the control group. The growth rate of the treatment groups was lower than that of the control group; the values at $T_{0.5}$ and $T_{2.0}$ levels were 87.21% and 68.18% of that of the control group, respectively. The energy consumption for adversity resistance was close to that of the control group under the low-concentration treatment groups, while the two high-concentration treatment groups showed higher energy consumption for adversity resistance than the control group.

After receiving treatment for 20 days, $T_{10.0}$ was excluded from the measurement. The net photosynthetic rate of the low-concentration treatment groups was close to 80% of that of the control group, while the value at $T_{4.0}$ level was 28.65% of that of the control group. The cellular metabolic energies of treatment groups were all lower than that of the control group, the values at $T_{0.5}$ and $T_{2.0}$ levels were 70.72% and 96.18% of that of the control group, respectively. The value at $T_{4.0}$ level showed less than 1% of that of the control group. The growth rates of the treatment groups were lower than that of the control group; the values at $T_{0.5}$ and $T_{2.0}$ levels were 88.14% and 50.61% of that of the control group, respectively. The energy consumptions for adversity resistance in the treatment groups were higher than that in the control group.

*3.7. Correlation Analysis of Photosynthetic Parameters and Cellular Metabolic Energy under Different NaHSO₃ Treatments*

The Pearson correlation coefficients for the relationship of the net photosynthetic rate ($P_N$), stomatal conductance (gs), transpiration rate (E), intercellular $CO_2$ concentration (Ci) and cellular metabolic energy ($\Delta G_B$) under different $NaHSO_3$ treatments are shown in Table 8. $P_N$ had a significant positive correlation with gs, E, Ci and $\Delta G_B$, gs was significantly correlated with E, Ci and $\Delta G_B$, and E was significantly correlated with Ci and $\Delta G_B$. However, Ci exhibited no significant correlation with $\Delta G_B$.

**Table 8.** Correlation between photosynthetic parameters and cellular metabolic energy under different $NaHSO_3$ treatments.

|  | **gs** | **E** | **Ci** | **$\Delta G_B$** |
|---|---|---|---|---|
| $P_N$ | 0.904 ** | 0.967 ** | 0.577 * | 0.813 ** |
| gs |  | 0.939 ** | 0.572 * | 0.645 ** |
| E |  |  | 0.635 * | 0.778 ** |
| Ci |  |  |  | 0.490 |

Note: Correlation significance level; *, ** indicates $p < 0.05$, $p < 0.01$, respectively (2-tailed).

## 4. Discussion

This paper mainly studied the effects of $NaHSO_3$ on the growth, photosynthesis and cellular metabolic energy of the aquatic plant *I. pseudocorus* and discussed the relationship mechanism between growth, photosynthesis and cellular metabolic energy in the process of plant development. The use of bisulfite-contaminated water for the planting and cultivation of plants may have adverse effects, but the impact of $NaHSO_3$ on plant photosynthesis or growth depends on its concentration, which may have a two-way impact. Previous studies have shown that $NaHSO_3$ treatment at low concentrations increased cyclic electron transfer around photosystem I, optimized the ATP/NADPH ratio and improved photosynthesis [38], and it can also be used as a nutrient element [39]. The sulfite sulfur is a potent oxygen acceptor which may also interfere with redox reactions [21], $NaHSO_3$ treatment at high concentrations was mainly shown to be an oxidant, resulting in excessive acidity and toxic effects on plants. According to the apparent phenomenon of this experiment, the addition of $NaHSO_3$ could reduce substance accumulation in *I. pseudocorus*, but plants grew well under a low concentration of $NaHSO_3$ (<2 mmol·L⁻¹), and a high concentration of $NaHSO_3$ (>4 mmol·L⁻¹) caused the plant to dry up and die. It was obvious that the

higher concentration of $NaHSO_3$ (>4 mmol·$L^{-1}$) inhibited the growth of *I. pseudocorus* leaves, but growth was inhibited first and then promoted under the low-concentration treatment (<2 mmol·$L^{-1}$). The number of leaves and tillers indicate that $NaHSO_3$ treatment of low concentration had no significant effect on plant growth but did reduce the ability of plant tillering. Severe damage appeared in *I. pseudocorus* leaves under high-concentration treatment. With the increase of $NaHSO_3$ concentration, plant growth, tillering and fresh matter accumulation were inhibited.

$NaHSO_3$ can be used as a photosynthetic promoter in agricultural production [18,19,39,40]. Results in other studies showed that 0.5 mmol·$L^{-1}$ $NaHSO_3$ was the optimal concentration to promote the photosynthetic oxygen release of *Anabaena*, and 1 mmol·$L^{-1}$ $NaHSO_3$ could increase the net photosynthetic rate of *Satsuma mandarin* by approximately 15% [20,41]. In general, a low concentration of $NaHSO_3$ (<1 mmol·$L^{-1}$) can significantly improve the photosynthetic oxygen release rate and dry matter accumulation of lower plants, such as algae [20,38,39], while most higher plants can significantly improve their photosynthetic carbon assimilation ability after being sprayed with $NaHSO_3$ (<8 mmol·$L^{-1}$) [18,19,41,42]. A high concentration of $NaHSO_3$ (>8 mmol·$L^{-1}$) has certain a toxicity to photosynthesis and other physiological processes in plants. $NaHSO_3$ (10 mmol·$L^{-1}$) significantly reduced the net photosynthetic rate of strawberry leaves [41]. High concentrations of sulfite inhibited photosynthetic electron transfer in pea leaves [43]. Bisulfite is also a sulfur source for plants, *Botryococcus braunii* stopped growing after 12 days in sulfur-free medium but grew well under bisulfite treatment at 0.1 or 0.8 mmol·$L^{-1}$ [39]. However, the addition of low concentrations of $NaHSO_3$ to promote plant growth works due to the supply of sulfur nutrition. Meanwhile, Kang et al. [19] showed that $NaHSO_3$ inhibited the photorespiration rate of *Caragana korshinskii*, and the glyoxylic acid content decreased significantly. The results of Wei et al. showed that $HSO_3^-$ could react with superoxide anion at photosystem I to produce $SO_4^{2-}$ [44], while Chen et al. [18] showed that a low concentration of $NaHSO_3$ increased the photosynthetic rate of soybean leaves, but the photorespiration rate also increased synchronously. Under normal conditions, photorespiration consumes approximately one quarter of the total photosynthetic yield, while higher temperatures, low $CO_2$ concentrations and stomatal closure, will increase Rubisco oxygenation beyond a flux beneficial for overall plant performance [45]. Therefore, the photosynthetic parameters of plants are of great significance when studying the effects of $NaHSO_3$ on plants.

When referring to the cellular metabolic energy, a high concentration of $NaHSO_3$ could have an adverse effect, whereas a low concentration of $NaHSO_3$ may have a favorable effect. In this paper, the cellular metabolic energy was calculated on the basis of electrical signals. Plant leaves of *I. pseudacorus* were investigated, and the equation of the cellular metabolic energy was jointly deduced according to the Gibbs free energy equation and the Nernst equation [46]. By substituting the parameters of the models for the changes of physiological capacitance, resistance and impedance with clamping force into the expression of cellular metabolic energy, the metabolic energy of different plant leaf cells in different environments can be quickly detected online without causing destruction [28]. At present, the existing studies reflect the metabolic energy of cells in vivo by using the intracellular energy charge state [47]. However, it cannot truly represent the metabolic energy of the plant cell solely by measuring the intracellular energy state. It is also difficult to measure the state of intracellular energy charge in vivo by current techniques. In this study, by measuring the electrophysiological indices of living leaves, the metabolic energy can be measured rapidly under different environments. Thus, the combination of the cellular metabolic energy and photosynthetic parameters can more accurately evaluate the growth status of plants.

The addition of $NaHSO_3$ could decrease the net photosynthetic rate of *I. pseudocorus*, the intercellular $CO_2$ concentration at $T_{0.5}$ level after the 10- and 20-day treatments and that at $T_{2.0}$ level after the 20-day treatment were all significantly higher than that of the control group. $NaHSO_3$ could inhibit the photosystem II activity and increase the respiration rate [20], and the proportional increase in photorespiration can be derived. The stomatal conductance of the low-concentration treatment groups was significantly lower than that

of the control group after 10 days, and higher than that of the control group after 20 days, which could also offer some support for this speculation. High-concentration $NaHSO_3$ treatment can destroy the structure of plant cell membrane by interfering with membrane proteins and lipids, bleach its chlorophyll and thus alter membrane integrity [20,21], therefore, under high-concentration ($T_{4.0}$, $T_{10.0}$) treatment, the cellular metabolic energy gradually decreased with the increase of treatment time, the net photosynthetic rate decreased, and the plants gradually dried up and died.

In addition, the growth of aquatic plants is greatly affected by environmental factors, among which the pH value is one of the most important traditional water quality indicators and one of the most important factors affecting nutrient absorption. A decrease in pH will be conducive to anion transmembrane transport and will have a relative effect on the inhibition of ion absorption, while an increase in pH will lead to the opposite effect [35]. Conversely, the absorption of nutrients by plants will also affect the pH value of the water environment. According to the degree of harm, acid rain was divided into three grades: $pH \leq 4.5$ was strong acid rain, $4.5 < pH \leq 5.6$ was weak acid rain and $pH > 5.6$ was normal [48]. In this study, from the average pH value in the treatment cycle, the control group and $T_{0.5}$ belonged to the normal range, $T_{2.0}$ was in the pH range of weak acid rain, and $T_{4.0}$ and $T_{10.0}$ were in the pH range of strong acid rain. The sulfur ions in the treatment solutions were absorbed by *Acorus calamus* L. during its growth. According to the total sulfur concentration, both $T_{0.5}$ and $T_{2.0}$ treatments promoted the sulfur absorption by *I. pseudocorus* compared with the control group, and $T_{0.5}$ had the best effect on promoting the absorption of sulfur. Combined with the value of $N_{WS}$ obtained by normalization, $T_{0.5}$ on the 10th day needed 0.1934 unit more energy than the control group to deal with the environment (adversity), and $T_{2.0}$ needed 0.0817 unit less energy than the control group, this was presumably because $T_{0.5}$ had a greater affinity to sulfur than $T_{2.0}$, and it needed more energy to absorb sulfur ions in the lower sulfur concentration solutions. It can be seen that the role that the $NaHSO_3$ in the low-concentration treatment groups plays in promoting the growth of *I. pseudocorus* is much greater than its toxic effect, so there is no need to allocate extra energy for *I. pseudocorus* to deal with adversity. $NaHSO_3$ at this concentration plays a role as a growth promoter to stimulate plant growth and energy storage. In the high-concentration treatment groups ($T_{4.0}$ and $T_{10.0}$), the absorption of sulfur was very low, which proved that $NaHSO_3$ had a toxic effect on *I. pseudocorus*.

## 5. Conclusions

Overall, there are significant differences between high-concentration and low-concentration $NaHSO_3$ treatment groups by growth, photosynthetic parameters or cellular metabolic energy, but the differences between each treatment group cannot be obtained. Combined with normalized treatment, the difference between each treatment group can be clearly seen. Under the hydroponic culture which contained $0.5 \ mmol \cdot L^{-1} \ NaHSO_3$, *I. pseudocorus* grew well and absorbed more sulfur as the measurement results of total sulfur content in treatment solutions. The results can provide simple and rapid solution for the cultivation of aquatic plants dealing with sulfur pollution, and dilution strategy can be set up to treat serious sulfur polluted water medium that is seriously polluted with sulfur.

**Data Availability Statement:** The datasets during or analyzed during the current study are available from the corresponding author upon reasonable request.

**Conflicts of Interest:** The authors declare no conflict of interest. The funders had no role in the design of the study.

## References

1. Gui, L.Y. Application of Plant Monitoring in Environmental Quality Assessment and Environmental Management. *Pollut. Control. Technol.* **2004**, *17*, 121–122. (In Chinese)
2. Pieters, O.; Swaef, T.D.; Lootens, P.; Stock, M.; Wyffels, F. Gloxinia—An Open-source Sensing Platform to Monivtor the Dynamic Responses of Plants. *Sensors* **2020**, *20*, 3055. [CrossRef]
3. Volkov, A.G.; Markin, V.S. Active and Passive Electrical Signaling in Plants. *Prog. Bot.* **2015**, *76*, 143–176. [CrossRef]
4. Fromm, J.; Lautner, S. Electrical signals and their physiological significance in plants. *Plant Cell Environ.* **2007**, *30*, 249–257. [CrossRef] [PubMed]
5. Sukhov, V.; Sukhova, E.; Vodeneev, V. Long-distance electrical signals as a link between the local action of stressors and the systemic physiological responses in higher plants. *Prog. Biophys. Mol. Biol.* **2019**, *146*, 63–84. [CrossRef] [PubMed]
6. Retivin, V.G.; Opritov, V.A.; Fedulina, S.B. Generation of action potentials induces preadaptation of *Cucurbita pepo* L. stem tissues to freezing injury. *Russ. J. Plant Physiol.* **1997**, *44*, 432–442.
7. Zhu, J.K. Abiotic Stress Signaling and Responses in Plants. *Cell* **2016**, *167*, 313–324. [CrossRef]
8. Liu, X.M.; Zhao, B.; Shen, H.F.; Xu, J.J.; Gao, X.N. Comprehensive Evaluation of Cold Resistance of Twenty Rhododendron Cultivars Under Cold Stress. *North. Hortic.* **2017**, *2017*, 60–66. (In Chinese)
9. Saglio, P.H.; Raymond, P.; Pradet, A. Metabolic Activity and Energy Charge of Excised Maize Root Tips under Anoxia. *Plant Physiol.* **1980**, *66*, 1053–1057. [CrossRef]
10. Vanhercke, T.; El, T.A.; Liu, Q.; Zhou, X.R.; Shrestha, P.; Divi, U.K. Metabolic engineering of biomass for high energy density: Oilseed-like triacylglycerol yields from plant leaves. *Plant Biotechnol. J.* **2014**, *12*, 231–239. [CrossRef]
11. Shu, S.M.; Duan, X.; Zhao, Y.Y.; Xiong, H.Q. A Model Based on Time, Space, Energy and Iterative Mechanism for Woody Plant Metabolic Rates and Biomass. *J. Biobased Mater. Bio.* **2016**, *10*, 184–194. [CrossRef]
12. Wang, H.X. *Pollution Ecology*, 2nd ed.; Beijing Higher Education Press: Beijing, China, 2002; pp. 173–179.
13. Nair, B.; Elmore, A.R. Final report on the safety assessment of sodium sulfite, potassium sulfite, ammonium sulfite, $NaHSO_3$, ammonium bisulfite, sodium metabisulfite and potassium metabisulfite. *Int. J. Toxicol.* **2003**, *22*, 63–68. [CrossRef] [PubMed]
14. Green, L.F. Sulphur dioxide and food preservation—A review. *Food Chem.* **1976**, *1*, 103–124. [CrossRef]
15. Gunnison, F.A. Sulphite toxicity: A critical review of in vitro and in vivo data. *Food Cosmet. Toxicol.* **1981**, *19*, 667–682. [CrossRef]
16. Bayat, L.; Askari-Mehrabadi, M.; Amini, F.; Morteza, Z.M. Effects of rhizobium inoculation on trifolium resupinatum antioxidant system under sulfur dioxide pollution. *Biol. J. Microorg.* **2014**, *2*, 37–50.
17. Galina, B.; Dmitry, Y.; Albert, B.; Vladislav, G.; Inna, K.G.; Aaron, F.; Rachel, A.; Robert, F.; Moshe, S. Sulfite oxidase activity is essential for normal sulfur, nitrogen and carbon metabolism in tomato leaves. *Plants* **2015**, *4*, 573–605. [CrossRef]
18. Chen, G.K.; Wang, X.Y.; Kang, H.J.; Sun, J. Effect of Different $NaHSO_3$ Concentrations on Gas Exchange and Fluorescence Parameters in Beans and Maize. *J. Nucl. Agric. Sci.* **2017**, *31*, 379–385. (In Chinese)
19. Kang, T.; Wu, H.D.; Lu, B.Y.; Luo, X.J.; Gong, C.M.; Bai, J. Low concentrations of glycine inhibit photorespiration and enhance the net rate of photosynthesis in *Caragana korshinskii*. *Photosynthetica* **2018**, *56*, 512–519. [CrossRef]
20. Wang, L.; Ming, C.; Wei, L.; Gao, F.; Lv, Z.; Wang, Q.; Ma, W. Treatment with moderate concentrations of $NaHSO_3$ enhances photobiological $H_2$ production in the cyanobacterium *Anabaena sp.* strain PCC7120. *Int. J. Hydrogen Energy* **2010**, *35*, 12777–12783. [CrossRef]
21. Lüttge, U.; Osmond, C.B.; Ball, E.; Brinckmann, E.; Kinze, G. Bisulfite compounds as metabolic inhibitors: Nonspecific effects on membranes. *Plant Cell Physiol.* **1972**, *13*, 505–514. [CrossRef]
22. Liu, N.; Lin, Z.F.; Guan, L.L.; Lin, Z.G.; Peng, C.L. Light acclimation and $HSO_3{}^-$ damage on photosynthetic apparatus of three subtropical forest species. *Ecotoxicology* **2009**, *18*, 929–938. [CrossRef]
23. Ryon, M.G.; Stewart, A.J.; Kszos, L.A.; Phipps, T.L. Impacts on streams from the use of sulfur-based compounds for dechlorinating industrial effluents. *Water Air Soil Pollut.* **2002**, *136*, 255–268. [CrossRef]
24. Meng, Z.Q.; Zhang, B. Polymerase chain reaction-based deletion screening of bisulfite (sulfur dioxide)-enhanced gpt-mutants in CHO-AS52 cells. *Mutat. Res. Fundam. Mol. Mech. Mutagenesis* **1999**, *425*, 81–85. [CrossRef]
25. Meng, Z.Q.; Zhang, L.Z. Cytogenetic damage induced in human lymphocytes by $NaHSO_3$. *Mutat. Res. Genet. Toxicol.* **1992**, *298*, 63–69. [CrossRef]
26. Hybská, H.; Lobotková, M.; Vanek, M.; Salva, J.; Veverková, D. Biomonitoring and its use in the assessment of the quality of wastewater treatment process. *Environ. Nanotechnol. Monit. Manag.* **2020**, *13*, 100292. [CrossRef]
27. Pandey, L.K.; Lavoie, I.; Morin, S.; Depuydt, S.; Jie, L.; Lee, H.; Jung, J.; Yeom, D.; Han, T.; Park, J. Toward a multibioassay-based index for toxicity assessment of fluvial waters. *Environ. Monit. Assess.* **2019**, *191*, 112. [CrossRef]
28. Wu, Y.Y.; Wu, Y.S.; Fang, L.; Wu, M.K.; Liu, C.Q. A Method for Determining the Cellular Metabolic Energy in Plant leaves. China Patent 2018107201885, 3 July 2018.

29. Solangi, K.A.; Wu, Y.; Chen, Q.; Qureshi, W.A.; Xing, D.; Tunio, M.H. The differential responses of *Aegiceras corniculatum* and *Kandelia candel* under salt stress and the re-watering phase. a study of leaf electrophysiological and growth parameters. *J. Plant Interact.* **2021**, *16*, 307–320. [CrossRef]

30. Zhang, L.Z.; Yang, F.P.; Jiang, X.Z.; Lan, X.H.; Ge, Z.Y. A Method for Determining the Total Sulfur in Water. China Patent 2015102633056, 21 May 2015.

31. Epstein, E.; Hagen, C.E. A kinetic study of the absorption of alkali cations by barley roots. *Plant Physiol.* **1952**, *27*, 457–474. [CrossRef]

32. Claassen, N.; Barber, S.A. A method for characterizing the relation between nutrient concentration and flux into roots of intact plants. *Plant Physiol.* **1974**, *54*, 564–568. [CrossRef]

33. Nielsen, N.E.; Barber, S.A. Differences among genotypes of corn in kinetics of P Uptake. *Agron. J.* **1978**, *70*, 695–698. [CrossRef]

34. Tang, Y.X.; Zheng, J.M.; Lou, L.P.; Zhang, Q.C. Comparisons of $NH_4^+$, $NO_3^-$ and $H_2PO_4^-$ uptake kinetics in three different macrophytes under waterlogged conditions. *Chin. J. Eco-Agric.* **2011**, *19*, 614–618. (In Chinese) [CrossRef]

35. Itoh, S.; Barber, S.A. Phosphorus uptake by six plant species as related to root hairs. *Agron. J.* **1983**, *75*, 457–461. [CrossRef]

36. Aksnes, D.L.; Egge, J.K. A theoretical-model for nutrient-uptake in phytoplankton. *Mar. Ecol. Prog. Ser.* **1991**, *70*, 65–72. [CrossRef]

37. Yang, Y.F.; Zhu, T.C. *Plant Ecology*, 2nd ed.; Higher Education Press: Beijing, China, 2011; pp. 202–203.

38. Wang, H.W.; Mi, H.L.; Ye, J.Y.; Deng, Y.; Shen, Y.K. Low concentrations of $NaHSO_3$ increase cyclic photophosphorylation and photosynthesis in cyanobacterium *Synechocystis* PCC6803. *Photosynth. Res.* **2003**, *75*, 151–159. [CrossRef]

39. Yang, S.; Wang, J.; Wei, C.; Cai, Z.; Fan, O. Effects of bisulfite and sulfite on the microalga *Botryococcus braunii*. *Enzym. Microb. Technol.* **2004**, *35*, 46–50. [CrossRef]

40. Tombuloglu, H.; Ablazov, A.; Filiz, E. Genome-wide analysis of response to low sulfur (LSU) genes in grass species and expression profiling of model grass species *Brachypodium distachyon* under S deficiency. *Turk. J. Biol.* **2016**, *40*, 934–943. [CrossRef]

41. Guo, Y.P.; Peng, Y.; Lin, M.L.; Guo, D.P.; Hu, M.J.; Shen, Y.K.; Zheng, S.J. Different pathways are involved in the enhancement of photosynthetic rate by $NaHSO_3$ and benzyladenine, a case study with strawberry (*Fragaria* × *Ananassa* Duch) plants. *Plant Growth Regul.* **2006**, *48*, 65–72. [CrossRef]

42. Guo, Y.P.; Hu, M.J.; Zhou, H.F.; Zhang, L.C.; Su, J.H.; Wang, H.W. Low concentrations of $NaHSO_3$ increase photosynthesis and biomass and attenuate photoinhibition in *Satsuma mandarin* (*Citrus unshiu* Marc.) plants. *Photosynthetica* **2006**, *44*, 333–337. [CrossRef]

43. Veeranjaneyulu, K.; Charlebois, D.; Soukpoé-Kossi, C.N.; Leblanc, R.M. Sulfite inhibition of photochemical activity of intact pea leaves. *Photosynth. Res.* **1992**, *34*, 271. [CrossRef]

44. Wei, L.; Yi, J.; Wang, L.; Huang, T.; Gao, F.; Wang, Q.; Ma, W. Light intensity is important for hydrogen production in $NaHSO_3$-treated *Chlamydomonas reinhardtii*. *Plant Cell Physiol.* **2017**, *58*, 451–457. [CrossRef] [PubMed]

45. Busch, F.A. Photorespiration in the context of Rubisco biochemistry, $CO_2$ diffusion and metabolism. *Plant J.* **2020**, *101*, 919–939. [CrossRef] [PubMed]

46. Deng, Z.X.; Li, C.C.; Wu, Y.Y. Comparison of Metabolic Energy in Two Mulberry Species Based on Leaf Electrophysiological Properties. *Earth Environ.* **2021**, *49*, 307–314. (In Chinese)

47. Hardie, D.G. AMPK: Positive and negative regulation, and its role in whole-body energy homeostasis. *Curr. Opin. Cell Biol.* **2015**, *33*, 1–7. [CrossRef] [PubMed]

48. Smith, W.H. *Air Pollution and Forests: Interactions between Air Contaminants and Forest Ecosystems*, 1st ed.; Springer: New York, NY, USA, 1981; pp. 84–106.